ChemComm

Accepted Manuscript

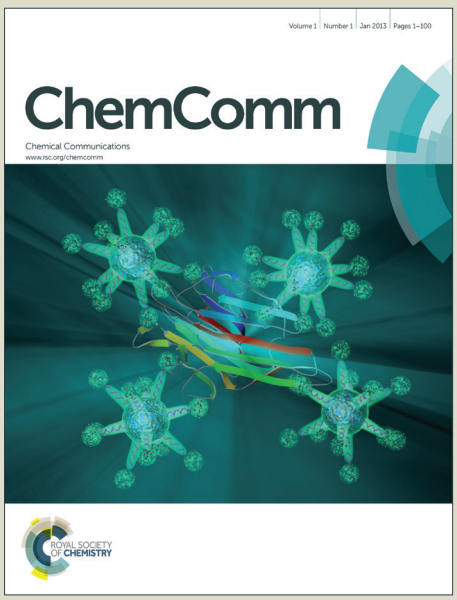

ROYAL SOCIETY OF CHEMISTRY

www.rsc.org/chemcomm

Journal Name

COMMUNICATION

Polymer@MOF@MOF: "Grafting From" Atom Transfer Radical Polymerization for the Synthesis of Hybrid Porous Solids

Received 00th January 20xx,
Accepted 00th January 20xx

DOI: 10.1039/x0xx00000x

www.rsc.org/

Kyle A. McDonald,[a] Jeremy I. Feldblyum,[b] Kyoungmoo Koh,[a] Antek G. Wong-Foy,[a] and Adam J. Matzger*[a,b]

The application of a core-shell architecture allows the formation of a polymer-coated metal-organic framework (MOF) maintaining high surface area (2289-2857 m^2g^{-1}). The growth of a MOF shell from a MOF core was used to spatially localize initiators by post-synthetic modification. The confinement of initiators ensures that polymerization is restricted to the outer shell of the MOF.

Zeolites, metal oxides, and activated carbons currently dominate industry-scale small molecule adsorption and separation applications;[1-4] combining these types of materials with polymers to form hybrid porous materials has the potential to enhance sorbent properties by combining the characteristics of inorganic and organic components.[5, 6] Organic-inorganic hybrid materials derived from grafting polymers to zeolites,[7] silica nanoparticles,[8] and carbon nanotubes,[9] for example, have received increasing attention in the past few years. These materials have shown promise in membrane mediated separations.[10, 11] However, compatibility between inorganic and organic components in hybrids can pose problems for the fabrication of functional and robust composites stemming from issues such as defects and poor polymer-inorganic adhesion.[11, 12] Metal-organic frameworks (MOFs), materials composed of metal clusters connected by organic bridging linkers, have tunable pore sizes/shapes and modular structures[13-16] that lend themselves to functionalization of the sort ideally suited to produce robust hybrid materials‡ that maintain excellent compatibility between MOF and polymer components.[12, 17] Recently, hybrid MOF materials have emerged, taking advantage of the porosity and tunability of MOFs to form composites with polymeric materials.[18-25] Many of the advancements that have been made in the realm of MOF-polymer composites have aimed to improve upon or combat some of the drawbacks of MOFs including poor processability and organic phase immiscibility. Grafting polymers from MOFs[23] or post synthetic polymerization to link MOF crystals together[18] are both promising routes to address these problems. However, the inclusion of polymers into MOF void space can be problematic for maximizing the accessibility of internal pores. Herein, polymer grafting and coating on MOFs is achieved by utilizing a core-shell architecture[26-29] that enables control over the extent to which polymer intrudes into the internal crystal pores. This strategy achieves polymer hybridization while maintaining the internal pore structure of the un-functionalized MOF.

A hybrid polymer-MOF architecture, polymer@MOF@MOF, in which polymer chains are covalently tethered to the outer shell of a core-shell MOF was targeted. Synthetic parameters were chosen with the goal of maintaining MOF rigidity and obtaining uniform polymer coverage on the surface of the MOF without substantially compromising internal porosity. In order to tether a polymer to a MOF, "grafting to" and "grafting from" approaches were considered as having the potential to yield the desired hybrid polymer-MOF.[30] "Grafting to" would involve the reaction of end-functionalized polymers with functional groups located on the MOF albeit with the risk that sterically bulky polymer chains might cause a decrease in the grafting density on the MOF. Therefore "grafting from" was chosen. This approach involves polymerization from active sites on the MOF, enabling the growth of polymer from initiator sites. Initiator sites can be incorporated onto the MOF by post-synthetic modification (PSM)[31] of a 2-aminoterephthalate linker with the carboxylic acid anhydride of the initiator for polymerization, thereby generating the tethered initiator. PSM of a MOF derived solely from 2-aminoterephthalate would result in initiator-carrying linker (and thus polymer) inclusion throughout the framework, thereby blocking significant amounts of pore space. To overcome this challenge, a core-shell architecture was utilized in which a shell of IRMOF-3, containing the 2-aminoterephthalate linker, was grown from the surface of MOF-5 to form IRMOF-3@MOF-5 (Figure 1a).[26, 27] MOF-5 was chosen because of its high surface area, reproducible synthesis, and broad use as a prototype system in the literature. Initiator carrying sites can be installed onto the IRMOF-3 outer shell by PSM.[31] This sequence enables formation of the initiator carrying linker selectively onto the outer shell for the polymerization of vinyl-type monomers. PSM was carried out by reaction of the amine groups of the IRMOF-3 shell with 2-bromoisobutyric anhydride and the resultant MOF is referred to as ICL@IRMOF-3@MOF-5 (initiator carrying linker@IRMOF-3@MOF-5, Figure 1b). With a MOF bearing a selectively placed polymerization initiator in hand, copper mediated Atom Transfer Radical Polymerization (ATRP)[32] was

† [a] Department of Chemistry, [b] Macromolecular Science and Engineering, University of Michigan, Ann Arbor, Michigan 48109-1055, USA
Email: Matzger@umich.edu
Electronic Supplementary Information (ESI) available: Synthesis and characterization. See DOI: 10.1039/x0xx00000x

carried out using methyl methacrylate (Figure 1c). The polymer@MOF@MOF materials, as exemplified by poly(methyl methacrylate)@IRMOF-3@MOF-5 (hereafter referred to as PMMA@IRMOF-3@MOF-5) is described here. PMMA@IRMOF-3@MOF-5 was washed thoroughly (see ESI) and activated under reduced pressure (~20 mTorr). Powder X-ray diffraction (PXRD) of MOF-5, IRMOF-3@MOF-5, ICL@IRMOF-3@MOF-5, and PMMA@IRMOF-3@MOF-5 demonstrates that the framework maintains its structure after shell formation, PSM, and polymer grafting (Figure S1 in ESI). Thermogravimetric analysis (TGA) of activated PMMA@IRMOF-3@MOF-5 reveals the depolymerization of PMMA at ~415 °C and subsequent degradation of MOF-5 at ~530 °C (Figure S7 in the ESI).

In order to determine the effects of functionalization and polymerization on the gas-accessible surface area of the core-shell MOF, the Brunauer-Emmett-Teller (BET) approximation was applied to data obtained from N_2 sorption experiments. The initial, activated MOF-5 isotherm (Figure 2) shows a surface area of 3530 m^2g^{-1}. The surface area of the ICL@IRMOF-3@MOF-5 is 3381 m^2g^{-1} indicating that the shell formation and functionalization occurs with minimal erosion of surface area. PMMA@IRMOF-3@MOF-5 displays a surface area of 2857 m^2g^{-1} after polymerization for 5 minutes and 2289 m^2g^{-1} after polymerization for 1 hour indicating that the MOF-5 core is intact and the porosity accessible. We hypothesize that the loss of surface area after polymerization is due primarily to the additional mass of the polymer, which does not contribute to the surface area. Thermogravimetric analysis of PMMA@IRMOF-3@MOF-5 shows the depolymerization of ~19 wt. % PMMA after polymerization for 5 minutes and ~23 wt. % PMMA after polymerization for 1 hour (Figure S7 in ESI), consistent with this notion although the observed further decrease in surface area of PMMA@IRMOF-3@MOF-5 after a longer polymerization time is also attributed to a greater role of the occupancy of the pore space by the growing polymer chains.

Understanding degree of polymerization and polymer molecular weight distribution (PDI) is necessary for optimization of the polymer segment properties and is expected to influence guest transport into the MOF core. In order to free the polymer chains from the MOF, hydrolysis of the framework is required. Although MOF-5 readily disintegrates in water, PMMA@IRMOF-3@MOF-5 crystals remain intact initially consistent with poor wetting behavior of these hydrophobic hybrids. However, treatment with 1M NaOH accompanied by intense shaking for several minutes, led to the disappearance of the PMMA@IRMOF-3@MOF-5 crystals. The polymer was then isolated by CH_2Cl_2 extraction. The ability to harvest the PMMA and determine molecular weight by gel permeation chromatography (GPC) was observed to be sensitive to digestion protocol; this is likely the result of a balance between

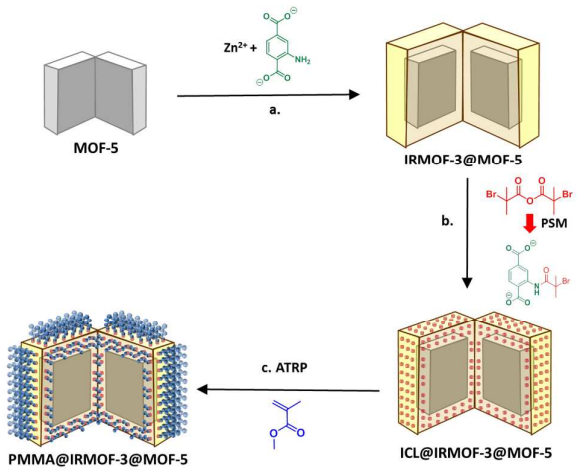

Fig. 1 Synthetic route to PMMA@IRMOF-3@MOF-5 wherein the cubic MOF crystal is represented as an open book to show both the core and shell chemistry: (a) core-shell formation on MOF-5 by growth of IRMOF-3 from MOF-5 seed crystals (IRMOF-3@MOF-5), (b) reaction of amine groups on the IRMOF-3 shell with 2-bromoisobutyric anhydride to generate initiator carrying linker@IRMOF-3@MOF-5 (ICL@IRMOF-3@MOF-5) and (c) ATRP on ICL@IRMOF-3@MOF-5 with methyl methacrylate to generate PMMA@IRMOF-3@MOF-5. See Electronic Supplementary Information (ESI) for experimental details.

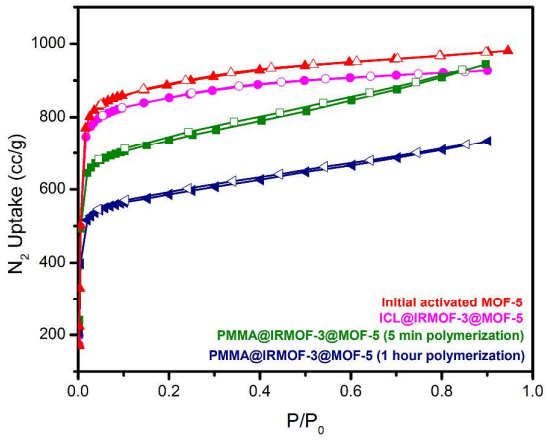

Fig. 2 N_2 sorption isotherms of MOF-5 (red), ICL@IRMOF-3@MOF-5 (pink), PMMA@IRMOF-3@MOF-5 after 5 minutes of polymerization at 65 °C (green), and PMMA@IRMOF-3@MOF-5 after 1 hour of polymerization at 65 °C (blue).

achieving complete framework degradation and avoiding extensive hydrolysis of the methyl ester side chains. GPC analysis found consistently high molecular weight polymer with narrow PDI (Mn = 421 kDa-615 kDa, PDI = 1.36-1.44. Figure S8 in the ESI). Initial results suggest that the molecular weight of the polymer does not increase linearly with time, which suggests that this is not a simple living polymerization without termination. To confirm that the polymerization depends on the presence of the initiator carrying functional group, polymerizations were conducted under identical conditions as those used to produce PMMA@IRMOF-3@MOF-5. The polymerization with IRMOF-3@MOF-5 and no copper catalyst resulted in no polymer grafted to the framework; the same result was found when using ICL@IRMOF-3@MOF-5. Therefore catalyst is necessary to initiate polymer grafting.

Raman microspectroscopy was applied to determine the depth of polymerization from the external surface of the MOF hybrid material. Single crystals were cleaved mechanically to expose the internal cross-section, and the intensity of the peak corresponding to the CH_2 stretch of the PMMA backbone was mapped as a function of the distance from the crystal surface (Figure 3). Raman mapping of PMMA@IRMOF-3@MOF-5 cross-sections demonstrate that the polymer extends to a depth of ~10 µm into the crystal. Furthermore, Raman mapping of freshly cut single crystals of IRMOF-3@MOF-5 (Figure S10 in ESI) demonstrates that the fluorescence background signal is much more pronounced in the IRMOF-3 shell (again extending ~10 µm into the MOF crystal); taken in combination these results demonstrate co-localization of shell and polymer consistent with the selective initiation of polymerization from the sites where the initiator-carrying linker is present. Hence, by modulating the thickness of the initiator-carrying shell, the thickness of the polymer film can likewise be controlled.

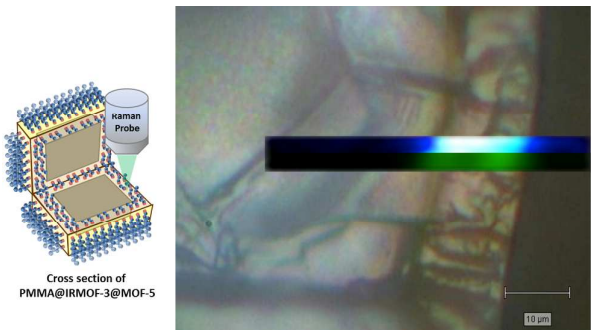

Fig. 3 Raman mapping of PMMA@IRMOF-3@MOF-5 showing the signal to baseline ratio of the peak between 787 and 818 cm^{-1} (blue), representative of the CH_2 stretch on the backbone of poly(methyl methacrylate), and showing the intensity at 741 cm^{-1} (green), which shows the fluorescence characteristic of the IRMOF-3 shell. Polymer and shell are co-localized.

Conclusions

PMMA@IRMOF-3@MOF-5, a hybrid polymer-MOF composite, was produced through a combination of core-shell and post-synthetic modification techniques. The use of core-shell architectures ultimately allows for polymer chains to be tethered to the outer shell of MOF-5, thereby, maintaining the inner porosity of the MOF. “Grafting from” using ATRP enables polymerization of PMMA on the outer shell of a MOF crystal, and opens the possibility to produce a complex polymer microstructure to modulate the accessibility of guests to a MOF.

This work was supported by Department of Energy (Award # DE-SC0004888). K. A. M. gratefully acknowledges support from the National Science Foundation Graduate Research Fellowship Program (NSF-GRFP). We would also like to thank Dr. Ping Guo for her assistance in synthesis and sorption related studies.

Notes and references

‡ In the literature simple MOFs have, on occasion, been referred to as hybrid materials, inconsistent with the common use of “hybrid” to indicate two or more phases intimately mixed typically on nanometer length scales. This is, however, more of an issue of connotation than denotation, as many common definitions of hybrid materials are so absurdly broad that they encompass ferrocene and copper acetate in spite of the fact that their properties do not arise in any simple fashion from phases of the pure metal and ligand. The use of the term hybrid materials for MOFs has recently been discouraged by IUPAC: Pure Appl. Chem. 2013; **85**, 1715.

1 W. Yuan, Y. S. Lin, W. Yang, *J. Am. Chem. Soc.* 2004, **126**, 4776.
2 R. M. de Vos, H. Verweij, *Science* 1998, **279**, 1710.
3 A.F. Ismail, L. I. B. David, *J. Membr. Sci.* 2001, **193**, 1.
4 S. Sircar, T. C. Golden, M. B. Rao, *Carbon* 1996, **34**, 1.
5 C. M. Zimmerman, A. Singh, W. J. Koros, *J. Membr. Sci.* 1997, **137**, 145.
6 A. C. Balazs, T. Emrick, T. P. Russell, *Science* 2006, **314**, 1107.
7 O. Celikbicak, G. Bayramoglu, M. Yılmaz, G. Ersoy, N. Bicak, B. Salih, M. Y. Arica, *Microporous Mesoporous Mater.* 2014, **199**, 57.
8 M. Sarsabili, M. Parvini, M. Salami-Kalajahi, P. Ganjeh-Anzabi, *Adv. Polym. Tech.* 2013, **32**, 21372.
9 H. Kong, C. Gao, D. Yan, *J. Am. Chem. Soc.* 2004, **126**, 412.
10 D. B. Mitzi, *Chem. Mater.* 2001, **13**, 3283.
11 J. Gascon, F. Kapteijn, B. Zornoza, V. Sebastián, C. Casado, J. Coronas, *Chem. Mater.* 2012, **24**, 2829.
12 H. Vinh-Thang, S. Kaliaguine, *Chem. Rev.* 2013, **113**, 4980.
13 S. L. James, *Chem. Soc. Rev.* 2003, **32**, 276.
14 M. Eddaoudi, J. Kim, N. Rosi, D. Vodak, J. Wachter, M. O'Keeffe, O. M. Yaghi, *Science* 2002, **295**, 469.
15 T.-H Park, K. Koh, A. G. Wong-Foy, A. J. Matzger, *Cryst. Growth Des.* 2011, **11**, 2059.
16 A. Dutta, A. G. Wong-Foy, A. J. Matzger, *Chem. Sci.* 2014, **5**, 3729.
17 S. Shahid, K. Nijmeijer, *J. Membr. Sci.* 2014, **470**, 166.
18 Y. Zhang, X. Feng, H. Li, Y. Chen, J. Zhao, S. Wang, L. Wang, B. Wang, *Angew. Chem. Int. Ed.* 2015, **54**, 4259.

19 J. Huo, M. Marcello, A. Garai, D. Bradshaw, *Adv. Mater.* 2013, **25**, 2717.
20 R. Zhang, S. Ji, N. Wang, L. Wang, G. Zhang, J.-R. Li, *Angew. Chem. Int. Ed.* 2014, **53**, 9775.
21 L. D. O'Neill, H. Zhang, D. Bradshaw, *J. Mater. Chem.* 2010, **20**, 5720.
22 D. Zhao, S. Tan, D. Yuan, W. Lu, Y. H. Rezenom, H. Jiang, L.-Q. Wang, H.-C. Zhou, *Adv. Mater.* 2011, **23**, 90.
23 H. Liu, H. Zhu, S. Zhu, *Macromol. Materi. Eng.* 2015, **300**, 191.
24 H. J. Lee, W. Cho, M. Oh, *Chem. Commun.* 2012, **48**, 221.
25 A.-L. Li, F. Ke, L.-G. Qiu, X. Jiang, Y.-M. Wang, X.-Y. Tian, *CrystEngComm* 2013, **15**, 3554.
26 K. Koh, A. G. Wong-Foy, A. J. Matzger, *Chem. Commun.* 2009, 6162.
27 K. M. Koh, A. G. Wong-Foy, A. J. Matzger, A. I. Benin, R. R. Willis., Block Coordination Copolymers. United States Patent US 8324323 B2, 2012
28 D. Zacher, R. Nayuk, R. Schweins, R. A. Fischer, K. Huber, *Cryst. Growth Des.* 2014, **14**, 4859.
29 P. Cubillas, M. W. Anderson, M. P. Attfield, *Cryst. Growth Des*. 2013, **13**, 4526.
30 K. Matyjaszewski, J. Xia, *Chem. Rev.* 2001, **101**, 2921.
31 Z. Wang, S. M. Cohen, *J. Am. Chem. Soc.* 2007, **129**, 12368.
32 K. Matyjaszewski, *Macromolecules* 2012, **45**, 4015.